Original Article

Modelling approaches to predict and evaluate schistosomiasis immunization utilizing SEA loaded on chitosan nanoparticles *via* liver tissue differentiation and angiogenesis

Samia E Etewa[1], Abd-Allah A Al-Hoot[2], Hesham M Sharaf[2], Howayda SF Moawad[1], Samira M Mohamed[1], Mahmoud A Alshafey[3], Huda H Senosy[2], Mohamed H Sarhan[1]

Departments of Medical Parasitology[1], Zoology[2] and Clinical Pathology[3], Faculties of Medicine[1,3], and Science[2], Zagazig University, Zagazig 44519, Egypt

ABSTRACT

Background: Anti-schistosome vaccination is a necessary approach to minimize the hepatic vascular changes that lead to hepatic pathological consequences.

Objective: To assess the prophylactic impact of soluble egg antigen (SEA) loaded on chitosan nanoparticles (ChNPs) on hepatic vascular and pathological consequences in experimental schistosomiasis.

Material and Methods: Seventy male Swiss albino mice were classified into 7 groups; each of 10. G1: Non-infected control; G2: Infected control group; G3: Injected by ChNPs then infected subcutaneously (SC) with *S. mansoni* cercaria; G4: Injected by Freund's Complete Adjuvant (FCA) then infected; G5: Injected by crude schistosomal egg antigen (SEA) combined with FCA (SEA-FCA) then infected; G6: Injected by SEA loaded on ChNPs (SEA-ChNPs) then infected; G7: Injected by both SEA-FCA + SEA-ChNPs then infected. Evaluation was done by parasitological, histopathological and immunohistochemical studies in murine models challenged by *Schistosoma mansoni* infection.

Results: SEA-ChNPs was more successful in reducing stools and liver egg counts, hepatic granulomas number and size, improving hepatic architecture and vasculature, minimizing hepatic fibrosis, enhancing angiogenesis constructive impact, ameliorating adverse effects during fibrogenesis and remodeling of hepatic tissue by fibrosis degradation than SEA-FCA.

Conclusion: ChNPs potentiated the protective and immune impact of SEA as proved by parasitological, histopathological and immunohistochemical assays; and confirmed its specific, marked, supportive and constructive effects on hepatic angiogenesis.

Keywords: angiogenesis; anti-schistosome vaccine; chitosan nanoparticles; hepatic architecture; hepatic vasculature, SEA.

List of abbreviations: AE: Encapsulation efficiency; **ANOVA:** Analysis of variance; **CAP:** Cercarial antigen preparation; **ChNPs:** Chitosan nanoparticles; **FCA:** Freund's complete adjuvant; **FGF2:** Fibroblast growth factor-2; **G:** Group; **H&E:** Hematoxylin & Eosin; **IACUC-ZU:** Institutional animal care and use committee-Zagazig University; **LC:** Loading capacity; **LSD:** Least significant difference; **MGD:** Mean granuloma diameter; **MGN:** Mean granulomas number; **MH:** Mayer's hematoxylin; **MSCs:** Mesenchymal stem cells; **MT:** Masson's trichrome; **NPs:** Nanoparticles; **PBS:** Phosphate-buffered saline; **PI:** Post infection; **R%:** Reduction percentage; **SC:** Subcutaneous; **SEA:** Soluble egg antigen; **SEA-ChNPs:** SEA loaded on ChNPs; **SEA-FCA:** Crude SEA combined with FCA; **SEM:** Scanning electron microscopy; **SWAP:** Soluble worm antigen preparation; **TBRI:** Theodor Bilharz Research Institute; **TPP:** Tripolyphosphate; **VEGF:** Vascular endothelial growth factor.

INTRODUCTION

Schistosomiasis is caused by blood flukes including all *Schistosoma* species. It affects about 207 million persons in 76 countries across the world, and is more prevalent in developing countries where about 800 million people are at the risk of schistosomiasis[1]. Following oviposition, schistosomes eggs that failed to exit with either urine or stools are carried back into the liver to be lodged in the pre-sinusoidal capillaries. The eggs are in intimate contact with the capillary endothelium before and during the generation of the granulomatous response[2]. *Schistosoma* miracidium inside the ovum secretes glycoprotein antigens that

pass through microscopic pores within the egg shell, so are called SEA. These antigens elicit a vigorous immune response that encapsulates the ova in pre-granuloma collagen fibers and immune cells, predominantly eosinophils and macrophages. The granuloma formation presents a barrier to sequester egg toxicity and antigenicity. Fibrosis of granulation tissues leads to disturbance of hepatic parenchymal architecture including its vasculature[3]. Despite portal vascular impairment, it was found that the total hepatic blood flow remained within normal limits with normal parenchymal cell perfusion, accompanied by absent gross changes in hepatic function tests. This was attributed to hepatic neovascular formation in the

areas of fibrosis to bypass occluded vessels as revealed by microcirculation studies specifically angiogenesis[4]. The latter is defined as the process of generation of new endothelial blood vessels from the already present post-capillary venules. It is a characteristic feature of both physiological and pathological processes as embryonic development, wound repair, inflammatory diseases and cancer[5]. Examples of angiogenesis inducers are the vascular endothelial growth factor (VEGF) and fibroblast growth factor-2 (FGF2)[6]. Schistosomiasis peri-portal fibrosis and peri-ovular granuloma formation are always accompanied by angiogenesis with prominent proliferation of neovascularization indicating fibrosis regression after curative therapy. However, in schistosomiasis, the resulting angiogenesis has double effects on fibrogenesis and fibrosis regression by allowing the detached pericytes from the capillary walls to recruit at the lesion's sites where they transform to myofibroblasts; while actin-containing pericytes help in remodeling of tissues and regression of post-curative fibrosis[7].

In spite of three decades of safe and effective use of chemotherapeutics, previous adverse impact of *Schistosoma* infection could not be avoided, specially on the liver; also prevalence of schistosomiasis is still high[8]. In addition, reinfection necessitates continuous retreatment which may allow the emergence of parasites resistant to chemotherapy, in addition to the difficulty of conveying treatment to all regions of endemic areas. So, immunization can be a necessary approach to complement chemotherapy in order to minimize the schistosomiasis hepatic vascular changes which are the key to the pathological consequences[9]. Immunization by antigens obtained from different schistosomal life cycle stages to induce protective immune response in mice was tested experimentally. One of those is SEA which is considered as a potential candidate for anti-schistosome vaccine[10]. It was emphasized that combining antigens with adjuvants increases vaccines potency[11,12]. However, a traditional adjuvant as FCA, may generally cause severe inflammation with unacceptable side effects[13]. This directed us to look for some modification of a potential candidate vaccine as SEA by using new techniques. With the introduction of nanotechnology in medical field studies, efforts to develop a new potent delivery vehicle for vaccines were initiated[14], drawing attention to the use of other adjuvants as ChNPs[15]. Among the tested polymers, nanospheres of ChNPs were endorsed for activating the immune response by enhancing the delivery of antigenic stimuli, in addition to its role as a non-specific anti-microbial agent[15,16]. It can be used as a vehicle for sure vaccine delivery and as a promising adjuvant for the potentiation of vaccine effects. The present research was applied to assess the prophylactic impact of SEA-ChNPs as a potential vaccine candidate, and to investigate its efficacy on the hepatic pathological consequences specifically the vascular changes in murine models after *Schistosoma* challenge.

MATERIAL AND METHODS

Study design: This case control study, began January 2017 and was completed December 2017. It was conducted at the laboratories of the Medical Parasitology and Pathology departments, Faculty of Medicine, Zagazig University and Theodor Bilharz Research Institute (TBRI), Imbaba, Giza, Egypt. Mice and cercariae were kindly supplied by Schistosome Biological Supply Center at TBRI.

Animals: The study was performed on 70 BALB/c male laboratory bred mice, eight weeks old, ± 20 grams weight, free of any parasitic infection. They were kept in sustained conditions of diet, water and animal house temperature of 20-22°C according to the international guidelines approved by the Institutional Animal Care and Use Committee, Zagazig University (IACUC-ZU).

Antigen: *Schistosoma* crude SEA was obtained from Schistosome Biological Supply Center, TBRI.

Adjuvant: FCA (Sigma Chemical Co., St Louis, Mo, USA) was emulsified in phosphate-buffered saline (PBS) at a ratio of 2:1.

Cecariae: *S. mansoni* cercariae (Egyptian strain) were obtained by the method described by Liang *et al.*[17] and used to experimentally infect mice by SC injection of ± 80 cercariae. All mice were euthanized 9 weeks post infection (PI).

ChNPs: Chitosan (degree of deacetylation 93%), sodium tripolyphosphate (TPP), PBS and acetic acid were purchased from Sigma–Aldrich, USA.

Preparation of antigens: Crude SEA was prepared[18], and the protein content was estimated using Bio-Rad kit (Bio-Rad Laboratories, Hercules, California, USA)[19]. The required concentration was adjusted with PBS to attain 50 µg/ml, and stored at -70°C until use.

ChNPs preparation[20]**:** Preparation was by ionic gelation method, i.e. the interaction of oppositely charged macromolecules. TPP has often been used to prepare ChNPs because TPP is nontoxic, multivalent and able to form gels through ionic interactions. The interaction can be controlled by the charge density of TPP and chitosan, which depends on the pH of the solution. Nanoparticles (NPs) were characterized by their size (mean size was 60.08 ± 2.009 nm), morphology (regular, rounded shape with a smooth surface) and surface charge, using advanced microscopic techniques as scanning electron microscopy (SEM) (JEOL 100 CX)[21]. These steps were performed by Nanotech Egypt Company, 6th October, Giza, Egypt.

Loading of antigen with ChNPs[16]**:** SEA-ChNPs was prepared by the addition of chitosan solution to TPP solution containing 100 mg/ml concentrations of SEA.

Loaded SEA was separated from aqueous suspension by centrifugation at 20,000 g at 14°C for 30 minutes. Protein content (free SEA) of the supernatant was calculated by the Bradford protein assay spectrophotometric method at 595 nm. The SEA encapsulation efficiency (%AE= [(A-B)/A] ×100) of NPs was calculated, where A is the total amount of SEA and B is the free amount of SEA.

Protocol of immunization[22,23]: Each mouse was first sensitized by an initial SC injection of 200 μl of the tested SEA, combined with FCA (groups 5 and 7), and with ChNPs (groups 6 and 7) with a total protein concentration of 30 μg. Two weeks later, another SC injection of 200 μl of the tested antigens after dilution to contain 20 μg protein was administered. FCA was combined with the crude SEA at 1:1 ratio and inoculated SC to the test groups 5 and 7; while ChNPs and FCA test groups (3 and 4 respectively) were injected SC by the same dose that was used in combination with the test antigens. Infection challenge of all tested mice was performed by SC injection of ±80 *S. mansoni* cercariae suspended in 0.2 ml distilled water, 3 weeks after the initial SC antigen injection. The suspension was injected by an insulin syringe SC[24]. The study groups are shown in the following table.

Study groups

Groups	Name	Immunization and challenge
G1	Non-infected control	Healthy control group
G2	Infected control	Infected SC with *S. mansoni* cercariae only
G3	ChNPs + infection	Received ChNPs then infected
G4	FCA + infection	Received FCA then infected
G5	SEA-FCA + infection	Received crude SEA combined with FCA then infected
G6	SEA-ChNPs + infection	Received SEA loaded on ChNPs then infected
G7	SEA-FCA + SEA-ChNPs + infection	Received both crude SEA combined with FCA + SEA loaded on ChNPs then infected

Immunization impact assessment: Immunization was assessed by parasitological, histopathological and immunohistochemical studies. Parasitological parameters included egg count/gram stools using modified Kato thick smear[25], hepatic egg count[26], and intestinal oogram pattern[27]. Hematoxylin and eosin (H&E) stain[28] was used to estimate reduction percentage in mean hepatic granuloma number (MGN)[29] and diameter (MGD)[30]. It was also used to determine granuloma tissue type (cellular, fibrocellular, or fibrous)[30] as well as to study inflammation degree of hepatic lobules[31] and hepatic vascular changes of the central vein, hepatic sinusoids and portal tract[32]. Masson's trichrome (MT) technique[33] was used to study schistosomiasis hepatic fibrosis qualitatively by microscopy as a descriptive study, and quantitatively by image analyzer. Four different stains were used; Weigert's iron hematoxylin for nuclei, picric acid for erythrocytes, a mixture of acid dyes (acid fuchsin-ponceau de xylidin) to color cytoplasm collagen light green. The percentage of fibrous tissue area was determined using OPTIKA image analyzer software. The MT-stained tissues showed blue coloration of fibrous tissue while sound hepatic parenchyma appeared red[34]. Immunohistochemical assay was carried out to study the hepatic vascular changes by detection of VEGF. The streptavidin–biotin immunoperoxidase technique (Dako-Cytomation, California, USA)[35] was used to stain 3-5 mm liver sections that were de-paraffinized in xylene and rehydrated in graded alcohol. Sections were boiled in citrate buffer (pH 6.0) for 20 min and then washed in PBS (pH 7.3). This was followed by blocking of endogenous peroxidase activity with 6% H_2O_2 in methanol. The sections were then incubated overnight with the VEGF anti mouse monoclonal antibodies (dilution 1: 200; Santa Cruz Biotechnology, California, USA), bathed five times in PBS, and then incubated with biotinylated goat anti-rabbit immunoglobulin. This was followed by a PBS wash and incubation with avidin–biotin complex for 1 h at room temperature. Product visualization was performed with diaminobenzidine substrate as chromogen. The sections were finally counterstained with Mayer's hematoxylin (MH). The criterion for a positive reaction confirming the presence of VEGF is a dark brownish intracytoplasmic precipitate. Cytoplasmic immunostaining for VEGF was semi-quantitatively scored as follows: 0, negative; +, mild (<10% expression of cells); ++, moderate (10–20% expression of cells); and +++, marked (expression >50%).

Statistical study: Collected data was coded and transferred into specially designed formats for computer feeding. Statistical Package for Social Sciences (SPSS) software (version 16 for windows) was utilized for descriptive measures including count, arithmetic mean and standard deviation (SD); one-way analysis of variance (*F*-test) (ANOVA) for normally quantitative variables to compare between more than two studied groups; student *t*-test to compare between means of different groups; post hoc testing using Fisher's least significant difference (LSD). *P* value <0.01 was considered statistically significant.

Ethics approval and consent to participate: All mice were reared and sacrificed according to the international guidelines approved by the Institutional Animal Care and Use Committee, Zagazig University.

RESULTS

Parasitological studies: Table (1) shows the impact of immunization using SEA-FCA and SEA-ChNPs on the egg count per gram stools and number of ova per gram liver. Significant reduction of *S. mansoni* eggs was recorded in fecal samples and liver tissue 9 weeks PI in G7 that received both SEA-FCA + SEA-ChNPs before infection, followed by G6 then G5 indicating that the most effective vaccine preparation was SEA-FCA + SEA-ChNPs followed by SEA-ChNPs, then SEA-FCA.

Remarkable oogram pattern changes were noted (Table 2) with significant reduction in mature and immature ova, and significant increase in dead ova in G7 (SEA-FCA+SEA-ChNPs then challenged); followed by G6

then G5, which indicates that the most effective vaccine was SEA-FCA+SEA-ChNPs followed by SEA-ChNPs, then SEA-FCA. Insignificant reduction in mature and immature ova was found in G3 and G4 with significant increase in dead ova in G3 (ChNPs only) compared to G2 (infected only).

Histopathological studies: It was observed that G7 (SEA-FCA+SEA-ChNPs then challenged) showed the most remarkable reduction in MGN and MGD followed by G6 then G5. Accordingly, SEA-FCA+SEA-ChNPs proved to be the most effective vaccine followed by SEA-ChNPs then SEA-FCA (Table 3). Table (4) showed significant reduction in the percentage of liver fibrosis in G7 followed by G6 then G5.

Table 1. *S. mansoni* eggs count in mice stools and liver tissues 9 weeks PI.

Groups		Eggs/gm stool	R%	Eggs/gm liver	R%
No.	Character	(Mean±SD)		(Mean±SD)	
2	Infection only	379.6 ± 36.1	-	1181.2 ± 43	-
3	ChNPs + infection	320.2 ± 16.3	15.6	961.1 ± 35.2	18.6
4	FCA + infection	329.9 ± 23.3	13.1	1006.3 ± 36	14.8
5	SEA-FCA + infection	181.8 ± 14.1	52.1	510.3 ± 26.9	56.8
6	SEA-ChNPs + infection	113.3 ± 18.5	70.2	329.7 ± 24.5	72.2
7	SEA-FCA + SEA-ChNPs + infection	91.8 ± 7.5	75.8	257.9 ± 17.2	78.2
	P value	<0.001*		<0.001*	

* Significant difference from infected control group, R%: Reduction percentage.

Table 2. Intestine oogram pattern of *S. mansoni* infected mice 9 weeks PI.

Groups		Immature	Mature	Dead
No.	Character	(Mean±SD)	(Mean±SD)	(Mean±SD)
2	Infection only	28.5 ± 3.4	65.3 ± 2.1	6.2 ± 0.8
3	ChNPs + infection	25.6 ± 5.6	62.1 ± 2.9	12.3 ± 2.6
4	FCA + infection	27.5 ± 3.2	64.4 ± 1.8	8.1 ± 2.3
5	SEA-FCA + infection	20.6 ± 2.6	43.7 ± 4.1	35.7 ± 2.7
6	SEA-ChNPs + infection	10.3 ± 1.7	24.3 ± 2.8	65.4 ± 3.1
7	SEA-FCA + SEA-ChNPs + infection	6.1 ± 1.2	13.2 ± 2.6	80.7 ± 4.2
	P value	<0.001*	<0.001*	<0.001*

* Significant difference from infected control group, R%: Reduction percentage.

Table 3. Granuloma number and diameter (size) of the tested groups.

Groups		Mean granuloma number	R%	Mean granuloma size	R%
No.	Character	(Mean±SD)		(Mean±SD)	
2	Infection only	71.6 ± 5.5	-	371.5 ± 32.3	-
3	ChNPs + infection	65.3 ± 7.4	8.8	332.8 ± 27.4	10.4
4	FCA + infection	68.1 ± 5.8	4.9	345.2 ± 29.8	7.1
5	SEA-FCA + infection	32.5 ± 6.1	54.6	250.9 ± 24.6	32.5
6	SEA-ChNPs + infection	24.9 ± 4.2	65.2	209.7 ± 20.1	43.6
7	SEA-FCA + SEA-ChNPs + infection	20.4 ± 4.3	71.5	158 ± 17.7	57.5
	P value	<0.001*		<0.001*	

* Significant difference from infected control group, R%: Reduction percentage.

Table 4. Percentage of hepatic fibrosis in infected mice groups.

Groups		Percentage of fibrosis (%)	R%
No.	Character	(Mean±SD)	
2	Infection only	37 ± 1.6	-
3	ChNPs + infection	30.9 ± 1.2	16.5
4	FCA + infection	33.2 ± 1.0	10.3
5	SEA-FCA + infection	19.7 ± 1.4	46.8
6	SEA-ChNPs + infection	15.3 ± 0.8	58.6
7	SEA-FCA + SEA-ChNPs + infection	12.6 ± 0.9	65.9
	P value	<0.001*	

* Significant difference from infected control group, R%: Reduction percentage.

Regarding changes in the liver parenchyma and vasculature in the tested mice groups, G7 showed mild central vein and hepatic sinusoids congestion with mild portal tract expansion and mild hepatic lobular inflammation. G5 and G6 showed moderate central vein and hepatic sinusoids congestion with moderate portal tract expansion and moderate hepatic lobular inflammation compared to the marked changes in G2, G3 and G4 (Table 5).

Liver sections of G1 (healthy control) showed normal liver architecture, normal central vein, hepatic sinusoids and portal tracts (Fig. 1), with normal collagen distribution within liver tissue (Fig. 2). Liver sections of G2 (infected only) showed multiple granulomas: cellular, fibrocellular and fibrous surrounding sound ova. Marked congested central veins and hepatic sinusoids with portal tract expansion and marked inter-lobular inflammation were seen with loss of normal

Table 5. Histopathological changes* of hepatic parenchyma and hepatic vasculature in the studied mice groups.

Groups	Central vein congestion	Hepatic sinusoids congestion	Portal tract expansion	Hepatic lobular inflammation
2	+++	+++	+++	+++
3	+++	+++	+++	+++
4	+++	+++	+++	+++
5	++	++	++	++
6	++	++	++	++
7	+	+	+	+

* +: mild; ++: moderate; +++: marked.

liver architecture (Fig. 3), as well as mild collagen deposition around the ova and thickening of the wall of portal tract blood vessels (Fig. 4). Liver sections of G3 (ChNPs+infection) showed multiple fibrocellular granulomas around more than one preserved ovum. Marked congestion and dilatation of central veins and hepatic sinusoids occurred with portal tract expansion and marked lobular inflammation around affected hepatocytes with loss of normal liver architecture (Figs.

5 and 6). Liver sections of G4 (FCA+infection) showed multiple cellular and fibrocellular granulomas, dilated and congested central veins and hepatic sinusoids with portal tract expansion; marked lobular inflammation, with loss of normal liver architecture (Figs. 7 and 8). Liver sections of G5 (SEA-FCA+infection) showed fibrocellular and fibrous granulomas around multiple ova surrounded by spaces, accompanied by moderate improvement of hepatic architecture with less
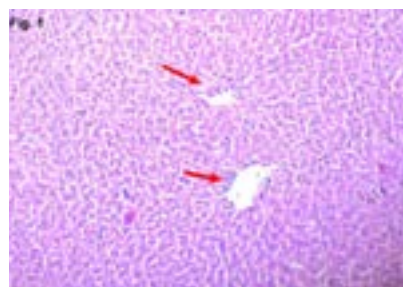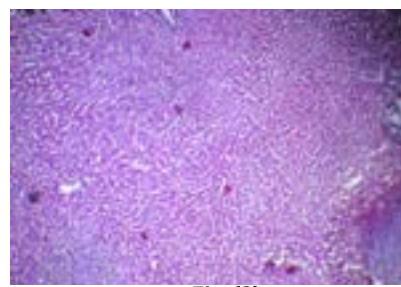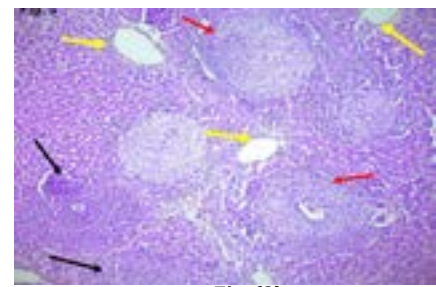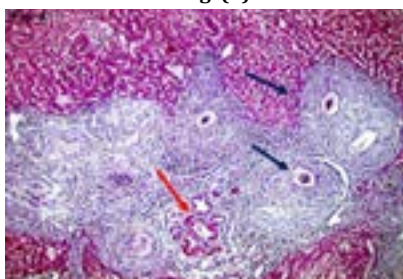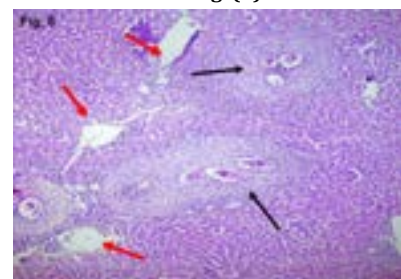
Fig. (1)   Fig. (2)   Fig. (3)
Fig. (4)   Fig. (5)   Fig. (6)
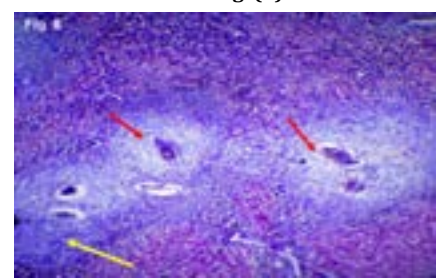
Liver of all tested groups sectioned and stained with Hematoxylin and Eosin (H&E) and Masson's trichrome (MT).
Fig. 1. G1 (healthy control) showed normal liver architecture (red arrows), normal central vein, hepatic sinusoids and portal tracts (H&E ×100).
Fig. 2. G1 (healthy control) showed normal collagen distribution within liver tissue (MT ×100).
Fig. 3. G2 (infected only) showed multiple granulomas: cellular (black arrow), fibrocellular and fibrous (red arrow) surrounding sound ova. Marked congested central veins (yellow arrows) and hepatic sinusoids with portal tract expansion and marked inter-lobular inflammation, hepatocytes in between were seen with loss of normal liver architecture (H&E ×100).
Fig. 4. G2 (infected only) showed multiple large sized fibrocellular granulomas surrounding intact ova (black arrows) with mild collagen deposition around the ova. Thickening of the wall of portal tract blood vessels (red arrow) (MT ×100).
Fig. 5. G3 (ChNPs + infection) showed multiple fibrocellular granulomas (black arrows) around more than one preserved ovum. Marked congestion and dilatation of central veins and hepatic sinusoids with portal tract expansion (red arrows) and marked lobular inflammation around affected hepatocytes with loss of normal liver architecture were noticed (H&E ×100).
Fig. 6. G3 (ChNPs + infection) showing many fibrocellular granulomas (red arrow) and cellular granuloma (yellow arrow) with sound ova in their centers and collagen deposition around the ova (MT×100).

expansion of portal tracts, central vein and hepatic sinusoids; moderate lobular inflammation was obvious (Fig. 9) with moderate collagen deposition (Fig. 10). Liver sections of G6 (SEA-ChNPs+infection) showed fewer numbers of fibrocellular and more fibrous granulomas with distorted ova. Hepatic architecture showed moderate improvement with lesser expansion of portal tracts, central vein and lobular inflammation (Fig. 11), and with more collagen deposition (Fig. 12). Liver sections of G7 (SEA-FCA+SEA-ChNPs+infection) revealed some distorted ova among other intact ova, and marked reduction in MGD was noticed. There was

marked improvement of hepatic architecture, portal tracts, central vein and hepatic sinusoids and mild lobular inflammation (Fig. 13) with more collagen deposition (Fig. 14).

Immunohistochemical studies of hepatic vascular changes: VEGF staining (index of angiogenesis) showed normal vascularity and architecture of the liver of the healthy control group G1. Brown colored VEGF was expressed in the vascular endothelial cells and sinusoidal endothelial cells (Fig. 15). In G2 (infected control), the endothelial cells, immunohistochemically
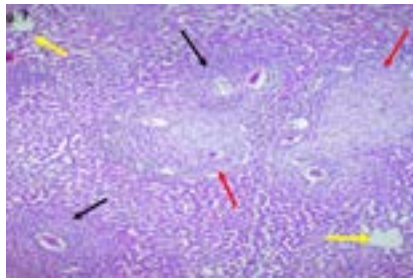
Fig. 7
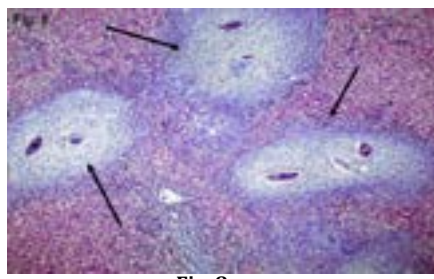
Fig. 8
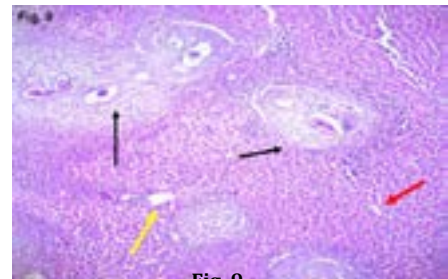
Fig. 9
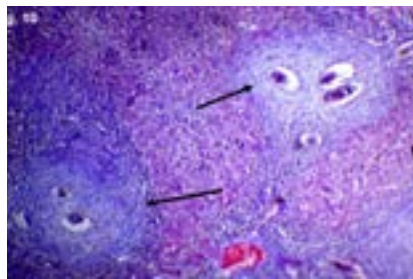
Fig. 10
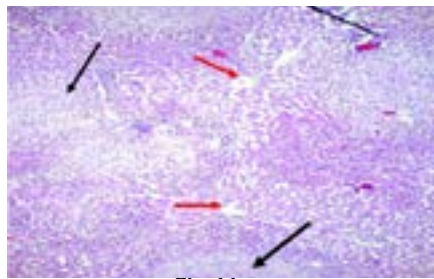
Fig. 11
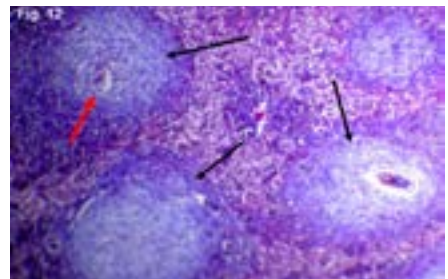
Fig. 12
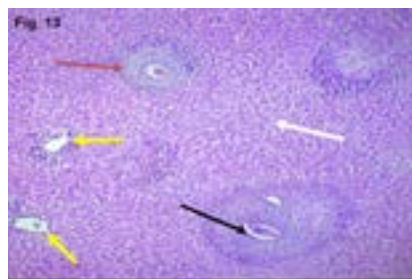
Fig. 13
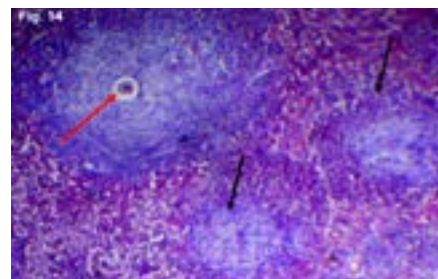
Fig. 14

Liver of all tested groups sectioned and stained with Hematoxylin and Eosin (H&E) and Masson's trichrome (MT).

Fig. 7. G4 (FCA + infection) showed multiple cellular (black arrows) and fibrocellular granulomas (red arrows), dilated and congested central veins and hepatic sinusoids with portal tract expansion (yellow arrows); marked lobular inflammation of hepatocytes, with loss of normal liver architecture (H&E ×100).

Fig. 8. G4 (FCA + infection) showed multiple fibrocellular granulomas (black arrows) with collagen deposition surrounding intact ova (MT ×100).

Fig. 9. G5 (SEA-FCA + infection) showed fibrocellular and fibrous granuloma (black arrows) around multiple ova which were surrounded by spaces, moderate improvement of hepatic architecture with less expansion of portal tracts, central vein and hepatic sinusoids (yellow arrow); moderate lobular inflammation of hepatocytes was obvious (red arrow) (H&E ×100).

Fig. 10. G5 (SEA-FCA + infection) showed multiple fibrocellular granulomas and fibrous granulomas with moderate collagen deposition (black arrows) (MT ×100).

Fig. 11. G6 (SEA-ChNPs + infection) showed fewer number of fibrocellular and more fibrous granulomas (black arrows) with distorted ova, moderate improvement of hepatic architecture with lesser expansion of portal tracts, central vein (red arrows) and lobular inflammation (H&E ×100).

Fig. 12. G6 (SEA-ChNPs + infection) showed fewer number of granulomas most of them were fibrocellular and fibrous (black arrows) with more collagen deposition and degenerated ova (red arrow) (MT ×100).

Fig. 13. G7 (SEA-FCA + SEA-ChNPs + infection) revealed some distorted ova (red arrow), some ova were intact (black arrow), marked reduction in granuloma size was noticed. There was marked improvement of hepatic architecture, portal tracts, central vein and hepatic sinusoids (yellow arrows) and mild lobular inflammation (white arrow) (H&E ×100).

Fig. 14. G7 (SEA-FCA + SEA-ChNPs + infection) showed an empty space around degenerated ova (red arrow) surrounded by fibrocellular granuloma and more collagen deposition (black arrow) (MT ×100).

identified by VEGF, were detected in great numbers within schistosome periovular granulomas. In other areas, there was fusion of several granulomas, while the proliferating small blood vessels appeared prominent in the inter-granulomatous tissue; the fibrous tissue assumed an angiomatoid appearance (Fig. 16). Moderate expression of VEGF was found in G3 (ChNPs+infection) with peripheral proliferating endothelial cells within fibrocellular *Schistosoma* granulomas containing intact ova (Fig. 17). Vascular proliferation formed vascular collars surrounding some granulomas in G4 (FCA+infection) (Fig. 18). In immunized then challenged groups, endothelial proliferation was detected by positive immunostaining of VEGF. This was quite evident within the involuting

granulomas and the vascularized areas of fibrosis; small patent new blood vessels were also seen within healed granulomas (Figs. 19-21). Group 5 (SEA-FCA+infection) showed moderate expression of VEGF and vascular proliferation within fibrocellular granulomas; small canalized blood vessels were seen a+t the periphery of the granuloma (Fig. 19). Group 6 (SEA-ChNPs+infection) showed marked expression of VEGF within and surrounding healed granulomas with intervening proliferating endothelial cells; small canalized blood vessels were seen within the granulomas (Fig. 20). G7 (SEA-FCA+SEA-ChNPs+infection) showed healed granulomas with marked expression of VEGF and proliferating endothelial cells; also, as well as canalization of granulomas by blood vessels (Fig. 21).
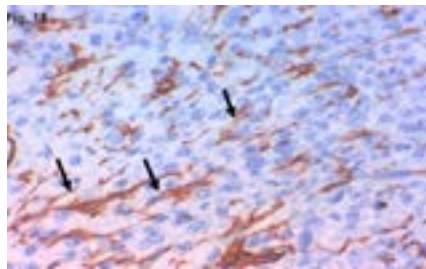
Fig. 15
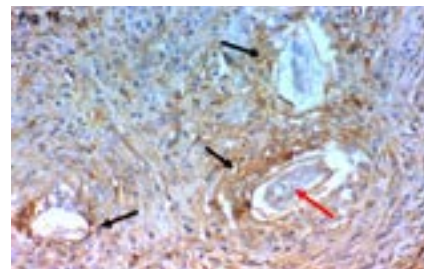
Fig. 16
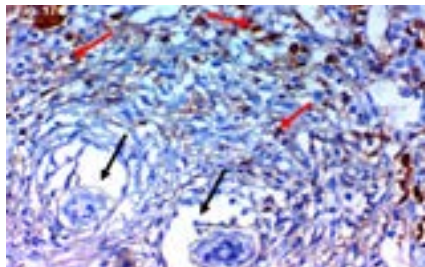
Fig. 17
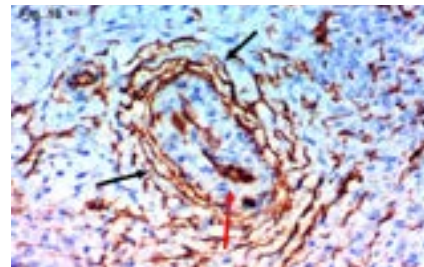
Fig. 18
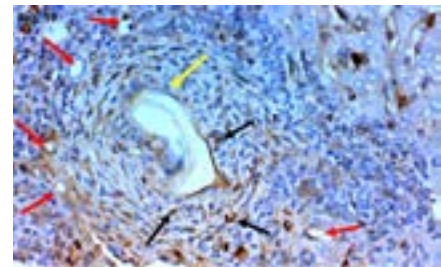
Fig. 19
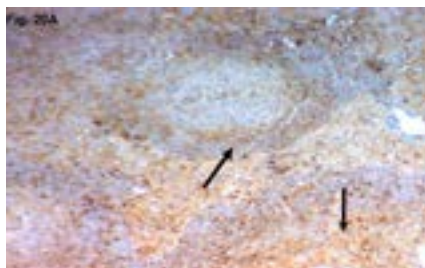
Fig. 20A
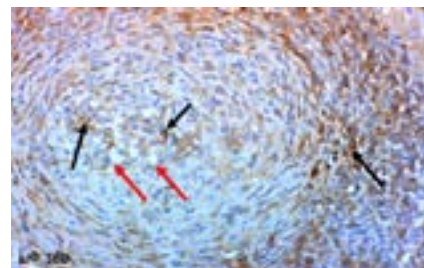
Fig. 20B
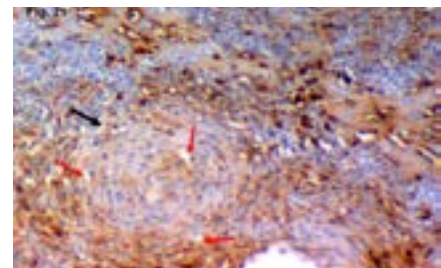
Fig. 21

Liver of all tested groups sectioned and immunohistochemically counter stained with Mayer's hematoxylin (MH)
Fig. 15. G1 (healthy control) showed normal murine liver vasculature with normal blood sinusoids expressed by brownish coloration (black arrows) (MH x400, VEGF).
Fig. 16. G2 (infected control) showed marked expression of VEGF (brownish coloration) in the inter-granulomatus tissue (black arrows) and proliferating endothelial cells within early cellular and fibrocellular *Schistosoma* granulomas (black arrows) with intact ova (red arrow) (MH x400, VEGF).
Fig. 17. G3 (ChNPs + infection) showed moderate expression of VEGF and peripheral proliferating endothelial cells (red arrows) within two fibrocellular *Schistosoma* granulomas with intact ova (black arrows) (MH x400, VEGF).
Fig. 18. G4 (FCA + infection) showed moderate expression of VEGF and proliferating endothelial cells within the granuloma, and at the periphery forming a vascular collar (black arrows) around *Schistosoma* granuloma (red arrow) (MH x400, VEGF).
Fig. 19. G5 (SEA-FCA + infection) showed moderate expression of VEGF and vascular proliferation (black arrows) within fibrocellular granuloma (yellow arrow), canalized small blood vessels were seen at the periphery of the granuloma (red arrows) (MH x400, VEGF).
Fig. 20. G6 (SEA-ChNPs + infection) showed marked expression of VEGF within and surrounding nearly healed granulomas with intervening proliferating endothelial cells (black arrows); small canalized blood vessels were seen within granuloma (red arrows) (MH x100 (A) and x400 (B), VEGF).
Fig. 21. G7 (SEA-FCA + SEA-ChNPs + infection) showed healed granuloma (black arrow) with marked expression of VEGF and proliferating endothelial cells; small canalized blood vessels were seen within granuloma (red arrows) (MH x400, VEGF).

DISCUSSION

Schistosomiasis is a life-threatening parasitic infection caused by blood dwelling flukes of the genus *Schistosoma*. It induces fatal liver fibrosis worldwide[36], causing a huge number of deaths annually[37]. Praziquantel chemotherapy eradicated the disease in many areas of the world but infection rates continue to be high in some endemic regions[38] which necessitates the implementation of a radical solution by preparation of suitable vaccines. In this regard, vaccination has a premium opportunity as it will combat non-reproducing worms inside the human body[39] leading to either decrease of the morbidity or the fecundity of schistosome worms. Thus reduction in worm numbers is the gold standard for anti-schistosome vaccine development. Knowing that schistosome eggs are responsible for both pathology and transmission, a schistosome vaccine targeting parasite fecundity and egg viability is also relevant[9]. It was advocated that the best long-term strategy to control schistosomiasis is through vaccination[40].

In the current work we used crude SEA as a potential anti-schistosomal immunization candidate. This was supported by the declaration of Khalifa *et al.*[41] that crude SEA was more heterogenous, being composed of twelve antigens that include multiple proteins, glycoproteins, and carbohydrates with glycolipids. Regarding antigenic efficacy, Affify[42] declared that SEA is superior to soluble worm antigen preparation (SWAP), and Etewa *et al.*[10] emphasized this superiority. The selection of a suitable adjuvant to help in stimulation of the appropriate immune response, is a critical step for development and employment of potent anti-schistosome vaccines[41]. The incorporation of an immunologically potent adjuvant would enhance and prolong qualified immune reactions to the used vaccines[43]. Despite wide use of FCA in the experimental vaccination studies, it was suspected to cause adverse complications for human health. Search for new adjuvants suitable for human applications was recommended in order to establish the safest formula for human vaccines[44].

Recently nanotechnology generated a potential impact in many fields such as medicine, pharmaceutics and engineering[45]. Nanostructures can cross the cell wall and tissue barriers as their particle size is very small, this makes them widely applicable in biomedical sciences[46]. Of note, a number of parasitological researches were conducted using ChNPs as carriers of drugs in treatment of parasitic diseases e.g. toxoplasmosis[47] and alveolar echinococcosis[48]. Also chitosan is soluble in diverse acids, is able to interact with polyanions to form complexes and gels, holds antibacterial and antifungal properties and is safe and nontoxic. All these characteristics render chitosan an ideal pharmaceutical vehicle that can be widely used in drug delivery[49]. In our study we experimentally tested ChNPs as carrier for a potential anti-schistosome vaccination candidate, SEA.

A significant reduction in the number of *S. mansoni* eggs in stools samples was detected 9 weeks PI in G7 that received both SEA-FCA + SEA-ChNPs then infected (Table 1). This may be attributed to the improved preservation of the SEA on ChNPs, thus potentiating and prolonging its efficacy. This result is substantiated by Gundersen *et al.*[50] who reported positive correlation between the number of eggs per gram stools and a high SEA level using tosyl-activated magnetic monodisperse particles coated with anti-circulating anodic antigen IgGl monoclonal antibody. The current results regarding crude SEA are mostly as those of Etewa *et al.*[51], who found significant reduction in the mean egg counts/g stools by Kato technique. The significant decrease of hepatic egg load in the same group (G7) vaccinated with both SEA-FCA+SEA-ChNPs, correlates with the previously reported significant percentage reduction of 89.5% using different antigens preparations composed of combined SWAP+SEA+FCA[51]. A lower record was attained by El-Ahwany *et al.*[52] who used SEA without FCA and by Rezende *et al.*[53] in a SWAP vaccinated model. They reported a percentage reduction in liver tissue egg load of 42.8% and 8.4%, respectively, which substantiates the higher protective effect of both SEA-FCA+SEA-ChNPs together with the augmenting role of the used adjuvants (FCA and ChNPs).

In our study, the most effective antigen combination resulting in remarkable oogram changes with significant decrease in mature and immature eggs and significant increase in dead eggs was SEA-FCA+SEA-ChNPs (G7) followed by SEA-ChNPs (G6), then SEA-FCA (G5) (Table 2).

A major pathology in schistosomiasis is the ova-induced hepatic granuloma, so, histopathological evaluations were of great importance in assessment of our work, depending on granulomas numbers, size and type, pathological events involving the central vein, liver sinusoids, portal tracts and liver lobules in murine hepatic tissues. Hepatic fibrosis percentages were investigated by image analysis of MT stained hepatic tissue sections with significant variation.

The reduction in number and size of liver granulomatous reaction may be attributed to SEA specific stimulation of immune reaction against *Schistosoma* eggs incriminated in hepatic pathology. This was obvious by the significant reduction of granuloma studied parameters using both SEA-FCA+SEA-ChNPs followed by SEA-ChNPs, then SEA-FCA with percentage decrease in number of hepatic granulomas 71.5%, 65.2% and 54.6% respectively and with percentage reductions in size of hepatic granulomas of 57.5%, 43.6% and 32.5% respectively (Table 3). This was associated with liver fibrosis

percentages which displayed significant reduction of 65.9%, 58.6% and 46.8% respectively in the same groups (Table 4). The reduction in the percentage of liver fibrosis propelled from 10.3% in G4 using infected mice immunized with FCA alone, to 46.8% in G5 using infected mice immunized with SEA-FCA with significant difference. These findings emphasized that SEA is a promising potential vaccine, especially when combined with either FCA or ChNPs as adjuvants, indicating that loading of SEA on ChNPs resulted in enhanced efficacy that dominated that of SEA with FCA. These results agree in part with those of Ismail[54] and Etewa *et al.*[10]. They endorsed the high immunogenicity of anti-schistosomal combined antigens (SEA+SWAP) as vaccination candidate for hepatic protection.

Currently, our findings are partially supported by those of Etewa *et al.*[55] who used different adjuvants preparations and found that the potent immunization which produced significant decrease of liver fibrosis and granuloma number and size, was SEA+ mesenchymal stem cells (MSCs) used as an adjuvant. Comparison revealed slight variation of percentage reductions, which may be attributed to the use of different adjuvants.

Liver sections of G2 (infected only) showed multiple large sized fibrocellular granulomas and intact ova surrounded by mild collagen deposition. In addition there was marked congestion of central veins and hepatic sinusoids with portal tract expansion, marked lobular inflammation and loss of normal liver architecture (Figs. 3 and 4). Liver sections of G7 (SEA-FCA + SEA-ChNPs followed by infection) showed fewer number and smaller size of granuloma; degenerated ova surrounded by empty spaces were enclosed in fibrocellular granulomas. Marked improvement of hepatic architecture, portal tracts, central veins and hepatic sinusoids were recorded in addition to mild lobular inflammation (Figs. 13 and 14). These signs of improvement are attributed to the efficient protective role of the potential vaccine when loaded on ChNPs. Gryseels *et al.*[39] revealed that hepatic granulomas surrounding schistosome eggs in experimentally infected mice were larger, with a cellular content mainly of eosinophils, lymphocytes, and some macrophages; but they later displayed shrinkage with more fibrous tissue deposition leading to retraction.

The findings of Alhusseiny *et al.*[31] and Abdel-Ghaffar *et al.*[32] supported our recorded notifications in table (5) that *Schistosoma* infection either alone (G2) or tested with ChNPs (G3) or FCA (G4) produced marked congestion of central veins and hepatic sinusoids, marked portal tract expansion and marked lobular inflammation. These hepatic vascular changes were explained by Silva *et al.*[56] who noted that in heavy infections, the peripheral portal vasculature becomes progressively amputated leading to increasing intra-portal pressure causing impaction of the new eggs in

the fine collateral veins emerging from larger portal vessels. Thus, portal vein branches of different calibers become partially or totally occluded. Additionally, arterial branches were increased in size and number with preserved normal hepatic veins.

Angiogenesis is a cascade process starting from extracellular matrix degradation followed by migration and proliferation of cells[57]. Two important types of cells are present in capillaries, endothelial cells and pericytes; a capillary cannot be formed in the absence of one of these cells[58]. Pericytes are contractile cells as they contain actin. They may be detached from the capillary walls and then assume the morphology and function of a myofibroblast, which can participate in the formation of the extra-cellular matrix. Fibrogenesis is associated with a strong proliferation of pericytes in the walls of capillaries and myofibroblasts in the interstitial tissues[59].

On the other hand, VEGF plays an essential role in angiogenesis[60]; it regulates vascular pathophysiology; including vasodilatation, vascular permeability, migration, and survival of endothelial cells[61]. It is an important indicator of progression of schistosomiasis pathology, as it reflects the angiogenesis that regulates the granulomas and fibrosis development in infected liver[62]. Our study documented the efficacy of different anti schistosomal vaccine preparations on the process of hepatic angiogenesis following schistosomiasis challenge. The process of angiogenesis was assessed by immunohistochemical staining using VEGF of liver tissues of different tested groups. The obtained results showed high expression of hepatic VEGF which appeared as dark brownish intracytoplasmic precipitates in *S. mansoni* infected mice. In some areas, when there was fusion of several granulomas, the proliferating small blood vessels appeared prominent in the inter-granulomatous tissue and the fibrous tissue assumed an angiomatoid appearance (Fig. 16). Vascular proliferation appeared to form vascular collars around some granulomas in the FCA immunized group (Fig. 18). These findings are supported by the results of Botros *et al.*[63] who reported that the VEGF immunoexpression in liver of *S. mansoni*- infected mice showed high expression of proliferating endothelial blood vessels. Apparently FCA alone had no specific role in our vaccination experiment, as emphasized by our results (Fig. 18) and as explained by Andrade and Santana[64]. The investigators reported that vascular proliferation can be observed throughout the early periovular granuloma formation, to be gradually displaced toward its periphery ending by forming of a surrounding vascular collar, while its center may appear almost avascular. Sometimes fusion of several granulomas occurs in periportal fibrosis during heavy infection both in man and experimentally, where the proliferating small blood vessels appear prominent in inter-granulomatous tissues and the fibrous tissue assumes an angiomatoid appearance which did not

occur in our vaccinated mice that received both SEA-FCA+SEA-ChNPs (G7) proving the potency of this combination.

In the vaccinated groups, endothelial proliferation within the involuting granulomas and the vascularized areas of fibrosis was quite evident. Also small patent new blood vessels were seen within healed granulomas (Figs. 19-21). Our results agree with Andrade[65] who noted that (angiogenesis) is a dominating feature in both fibrogenesis and fibrolysis which are constant and important features occurring during the pathology of schistosomiasis. This means that angiogenesis has a double and paradoxical role during schistosomiasis. These opposite effects were directed by the disease sequence of morbidity and chronicity which may form an obstacle to the constructive effect of angiogenesis. Our results confirmed the participation of angiogenesis process not only in the formation of hepatic schistosomal granulomas but also in the evolution following anti-schistosome vaccination. In addition, the present findings showed that fibrosis regression occurring after vaccination, as evidenced by image analysis of hepatic tissue stained by MT stain, is associated with considerable vascular remodeling. These results are in accordance with Andrade *et al.*[7] and Abdel Fattah and Ahmed[66].

Our work highlighted the potentiality and potency of our tested vaccines preparation loaded on ChNPs as translated by the reduction of egg counts and the findings of oogram pattern which supported the current immunohistochemical results where *S. mansoni* egg antigens induced angiogenesis-related reactions by stimulating VEGF in endothelial cells, this was illustrated by many focal areas of vascular proliferation, evident by positive staining for VEGF[67]. Adherence of schistosomes ova to endothelial cells of blood vessels allows them to alter their shape, break their surrounding basement membrane, proliferate, and migrate increasing angiogenesis[6].

In conclusion, the obtained parasitological and histopathological findings highlighted the effective and protective effects of SEA-ChNPs. It is a promising new preparation of antigens to be used in immunization against schistosomiasis. In addition, it is concluded that angiogenesis as expressed immunohistochemically by hepatic VEGF, may synergize then antagonize hepatic affection by schistosomiasis. Angiogenesis is a double-edged weapon, so could it be used to protect the hepatic tissues only? Hence, further trials are recommended to mask and ameliorate adverse effects of infection by immunization or by therapeutic drugs preparations that may enhance angiogenesis protective and constructive role in the liver during schistosomiasis. So, the stimulation and recruitment of the immune responses could be mediated by new preparations of drugs and/or vaccines depending on nanotechnology as an example.

REFERENCES

1. Shariati-Sharifi F, Muro A. Effects of *Schistosoma bovis* on angiogenesis factor expression in macrophage cells of rats. J Babol Univ Med Sci 2016; 18: 61-66.
2. Lenzi HL, Sobral AC, Lenzi JA. Participation of endothelial cells in murine schistosomiasis. Braz J Med Biol Res 1988; 21: 999-1003.
3. Hams E, Aviello G, Fallon PG. The *Schistosoma* granuloma: friend or foe? Front Immunol 2013; 4: 1–8.
4. Warren KS. Hepatosplenic schistosomiasis: a great neglected disease of the liver. Gut 1978; 19: 572-577.
5. Carmeliet P, Jain RK. Angiogenesis in cancer and other diseases. Nature 2000; 407: 249–257.
6. Loeffler DA, Lundy SK, Singh KP, Gerard HC, Hudson AP, Boros DL. Soluble egg antigens from *Schistosoma mansoni* induce angiogenesis-related processes by up-regulating vascular endothelial growth factor in human endothelial cells. J Infect Dis 2002; 185: 1650–1656.
7. Andrade ZA, Baptista AP, Santana TS. Remodeling of hepatic vascular changes after specific chemotherapy of schistosomal periportal fibrosis. Mem Inst Oswaldo Cruz 2006; 101: 267–272.
8. King CH. Lifting the burden of schistosomiasis-defining elements of infection-associated disease and the benefits of antiparasite treatment. J Infect Dis 2007; 196: 653–655.
9. McManus DP, Loukas A. Current status of vaccines for schistosomiasis. Clin Microbiol Rev 2008; 21: 225-242.
10. Etewa SE, Hegab MH, Metwally AS, Abd Allah SH, Shalaby SM, El-Shal AS, *et al.* Murine hepatocytes DNA changes as an assessment of the immunogenicity of potential anti-schistosomal vaccines experimentally. J Parasit Dis 2017; 41: 219–229.
11. Palatnik-de-Sousa CB. Vaccines for leishmaniasis in the fore coming 25 years. Vaccine 2008; 26: 1709-1724.

12. Etewa SE, Al-Hoot AA, Sharaf HM, Mohammad SM, Moawad HSF, Sarhan MH, *et al.* A potential prophylactic strategy of anti-schistosomal immunization using nanotechnology in murine models. PUJ 2018; 11: 162-174.

13. Handman E. Leishmaniasis: current status of vaccine development. Clin Microbiol Rev 2001; 14: 229-243.

14. Gregory AE, Titball R, Williamson D. Vaccine delivery using nanoparticles. Front Cell Infect Microbiol 2013, 3: 1-13.

15. Bowman K, Leong KW. Chitosan nanoparticles for oral drug and gene delivery. Int J Nanomed 2006, 1: 117–128.

16. Danesh-Bahreini MA, Shokri J, Samiei A, Kamali-Sarvestani E, Barzegar Jalali M, Mohammadi-Samani S. Nanovaccine for leishmaniasis: preparation of chitosan nanoparticles containing *Leishmania* superoxide dismutase and evaluation of its immunogenicity in BALB/c mice. Int J Nanomed 2011, 6: 835-842.

17. Liang YS, John I, Bruce JI, David AB. Laboratory cultivation of schistosome vector snails and maintenance of schistosome life cycle. Proc First Sine Am Symp 1987; 1: 34.

18. Boros DL, Warren KS. Delayed hypersensitivity type III: granuloma formation and dermal reaction induced and elicited by a soluble factor isolated from *Schistosoma mansoni* eggs. J Exp Med 1970; 132: 488-507.

19. Bradford MM. A rapid and sensitive method for the quantitation of microgram quantities of protein utilizing the principle of protein-dye binding. Anal Biochem 1976; 72: 248-254.

20. Hrkach J, Von Hoff D, Ali MM, Rianova E, Auer J, Campbell T, *et al.* Preclinical development and clinical translation of a PSMA-targeted docetaxel nanoparticle with a differentiated pharmacological profile. Sci Transl Med 2012; 4: 128-139.

21. Pal SL, Jana U, Manna PK, Mohanta GP, Manavalan R. Nanoparticle: An overview of preparation and characterization (2000-2010). J Appl Pharm Sci 2011; 1: 228-234.

22. Nabih I, Soliman AM. Studies on fresh water snails, specific intermediate host for schistosomiasis. II. Isolation of total protein from native and irradiated snails. Cell Mol Biol 1986; 32: 315- 317.

23. Smithers SR, Hackett F, Ali OP, Simpson AJG. Protective immunization of mice against *Schistosoma mansoni* with purified adult worm surface membranes. Parasite Immunol 1989; 11: 301-318.

24. Peters AP, Warren KS. A rapid method of infecting mice and other laboratory animals with *Schistosoma mansoni* subcutaneous injection. J Parasitol 1969; 55: 558- 563.

25. Martin LK, Beaver PC. Evaluation of kato thick-smear technique for quantitative diagnosis of helminth infection. Am J Trop Med Hyg 1968; 17: 382-91.

26. Cheever AW. Postmortem study of schistosomiasis manosni in man. Am J Trop Med Hyg 1968; 17: 38-64.

27. Pellegrino J, Oliveira CA, Faria J, Cunha AS. New approach to the screening of drugs in experimental schistosomiasis *mansoni* in mice. Am J Trop Med Hyg 1962; 11: 201-215.

28. Von Lichtenberg FC. Host response to eggs of *Schistosoma mansoni*. I Granuloma formation in the sensitized laboratory mouse. Am J Pathol 1962; 41: 711-731.

29. Ali SA, Hamed MA. Effect of *Ailanthus altissima* and *Zizyphus spina-christi* on bilharzial infestation in mice: histological and histopathological studies. J Applied Sci 2006; 6: 1437-1446.

30. Romeih MH, Hassan HM, Shousha TS, Saber MA. Immunization against Egyptian *Schistosoma mansoni* infection by multivalent DNA vaccine. Acta Biochim Biophys Sin (Shanghai) 2008; 40: 327-338.

31. Alhusseiny SM, El-Beshbishi SN, Abu Hashim MM, El-nemr HE, Handoussa A. A comparative study on the anti schistosomal and hepatoprotective effects of vinpocetine and isosorbide-5 mononitrate on *Schistosoma mansoni* infected mice. Acta Tropica 2017; 176: 114–125.

32. Abdel Ghaffar MM, Saad AE, Moharm IM, Sharaf OF, Badr MT, Ibrahim AF. Parasitological and histopathological effects of some antischistosome drugs in *Schistosoma mansoni* infected mice. MMJ 2018; 30: 1193–1202.

33. Bancroft S, Stevens A. Theory and practice of histological techniques, 2nd ed. Churchill-Livingston, New York; 1982.

34. Marie NA, Helmy DO, Badawi MA, Farrag AH, Soliman ASA. Image analysis assessment of fibrosis from liver biopsy of chronic hepatitis patients. J Arab Soc Med Res 2012; 7: 48–56.

35. Soo R, Putti T, Tao Q, Goh BC, Lee KH, Kwok-Seng L, *et al.* Over expression of cyclooxygenase-2 in nasopharyngeal carcinoma and association with epidermal growth factor receptor expression. Arch Otolaryngol Head Neck Surg 2005; 131: 147–152.

36. Richter J, Bode JG, Blondin D, Kircheis G, Kubitz R, Holtfreter MC, *et al.* Severe liver fibrosis caused by *Schistosoma mansoni*: management and treatment with a transjugular intrahepatic portosystemic shunt. Lancet Infect Dis 2015; 15: 731–737.

37. WHO. Schistosomiasis fact sheet. Updated April 17, 2019. Available at: http://www.who.int/news-room/fact-sheets/detail/schistosomiasis. Accessed August 2, 2019.

38. Gray DJ, McManus DP, Li YS, Williams GM, Bergquist R, Ross AG. Schistosomiasis elimination: lessons from the past guide the future. Lancet Infect Dis 2010; 10: 733-736.

39. Gryseels B, Polman K, Clerinx J, Kestens L. Human schistosomiasis. Lancet 2006; 36: 1106-1118.

40. WHO. Schistosomiasis: population requiring preventive chemotherapy and number of people

treated in 2010. Weekly Epidemiol Rec 2012; 87: 37-44.

41. Khalifa RMA, Elnadi NA, Omran EK, Abdel-Tawab RA. Immunological response and the probability of production of vaccine for schistosome parasites. Egypt J Med Sci 2011; 32: 547-570.

42. Affify HA. Detection of circulating schistosomal antigens in serum and urine samples in patients with schistosomiasis. MD Thesis, Zagazig University, Egypt, 1999.

43. Vogel FR. Improving vaccine performance with adjuvants. Clin Infect Dis 2000; 30: 266-270.

44. Hacariz O, Sayers G, McCullough M, Garrett M, O'Donovan J, Mulcahy G. The effect of quil adjuvant on the course of experimental *Fasciola hepatica* infection in sheep. Vaccine 2009; 27: 45-50.

45. Lanka D, Mittapally VK. Preparation and Applications of Chitosan Nanoparticles: A Brief Review. Res Rev J Material Sci 2016; https://doi.org/10.4172/2321-6212.1000r001.

46. Dou Z, Wang G, Zhang E, Ning F, Zhu Q, Jiang J, *et al.* Effect of Al2O3 nanoparticles doping on the microwave dielectric properties of CTLA ceramics. J Material Sci Eng 2016; 5(4): 1000256.

47. Etewa SE, Abo El-Maaty DA, Hamza RS, Metwaly AS, Sarhan MH, Abdel-Rahman SA, *et al.* Assessment of spiramycin-loaded chitosan nanoparticles treatment on acute and chronic toxoplasmosis in mice. J Parasit Dis 2018; 42: 102–113.

48. Abulaihaiti M, Wu XW, Qiao L, Lv HL, Zhang HW, Aduwayi N, *et al.* Efficacy of Albendazole-Chitosan microsphere-based treatment for alveolar echinococcosis in mice. PLoS Negl Trop Dis 2015; 9:e0003950.

49. Kean T, Thanou M. Biodegradation, biodistribution and toxicity of chitosan. Adv Drug Deliv Rev 2010; 62: 3–11.

50. Gundersen SG, Hagensen I, Jonassen TO, Figenschau KJ, de Jonge N, Deelder AM. Magnetic bead antigen capure enzyme linked immunoassay in microtitre trays for rapid detection of schistosomal circulating anodic antigen. J Immunol Meth 1992; 148: 1-10.

51. Etewa SE, Hegab MH, Metwally AS, Abd Allah SH, Shalaby SM, El-Shal AS, *et al.* A molecular approach for evaluation of experimental trials of anti schistosomal vaccination in murine models. Afro-Egypt J Infect Endem Dis 2016a; 6: 142-151

52. El-Ahwany E, Bauiomy IR, Nagy F, Zalat R, Mahmoud O, Zada S. Regulatory cell responses to immunization with a soluble egg antigen in *Schistosoma mansoni* infected mice. Korean J Parasitol 2012; 50: 29-35.

53. Rezende CMF, Silva MR, Santos IGD, Silva GAB, Gomesa DA, Goesa AM. Immunization with rP22 induces protective immunity against *Schistosoma mansoni*: Effects on granuloma down-modulation and cytokine production. Immunol Lett 2011; 141: 123-133.

54. Ismail OA. Study of the efficacy of adult worm, cercarial and egg antigens in protection against experimental intestinal schistosomiasis. MD Thesis, Suez Canal University, Egypt, 2005.

55. Etewa SE, Abd Allah SH, Badawey MS, Shalaby SM, El-Shal AS, El-Shafey MA, *et al.* The effect of stem cells as an adjuvant on the immunogenicity of a potential anti-schistosomal vaccine in mice. J Egypt Soc Parasitol 2016b; 46: 693-716.

56. Silva LM, Ribeiro-Dos-Santos R, Soares MB, Andrade ZA. Characterization of the vascular changes in schistosomal portal (pipestem) fibrosis of mice. Acta Tropica 2006; 98: 34-42.

57. Ono M. Molecular links between tumor angiogenesis and inflammation: inflammatory stimuli macrophages and cancer cells as targets for therapeutic strategy. Cancer Science 2008; 99: 1501–1506.

58. Bergers G, Song S. The role of pericytes in blood-vessel formation and maintenance. Neuro Oncol 2005; 7: 452-464.

59. Eyden B. The myofibroblast: a study of normal, reactive and neroplastic tissues, with an emphasis on ultrastructure. Part 1 – Normal and reactive cells. J Submicrosc Cytol Pathol 2005; 37: 109-204.

60. Li S, Ren W, Li W, Zhao N, Ma G, Gong P, *et al.* A shift to Th2 immune response caused by constitutive expression of IPSE/alpha-1 in transfected pig fibroblasts in mice. Vet Immunol Immunopathol 2013; 152: 269-276.

61. Franchitto A, Onori P, Renzi A, Carpino G, Mancinelli R, Alvaro D, *et al.* Expression of vascular endothelial growth factors and their receptors by hepatic progenitor cells in human liver diseases. Hepatobiliary Surg Nutr 2013; 2: 68-77.

62. Shariati F, Pérez-Arellano JL, Carranza C, López-Abán J, Vicente B, Arefi M, *et al.* Evaluation of the role of angiogenic factors in the pathogenesis of schistosomiasis. Exp Parasitol 2011; 128: 44-9.

63. Botros SS, Hammam M, Bergquist R. Praziquantel efficacy in mice infected with PZQ non-susceptible *S. mansoni* isolate treated with artemether: parasitological, biochemical and immunohistochemical assessment. APMIS 2010; 118: 692–702.

64. Andrade ZA, Santana TS. Angiogenesis and schistosomiasis. Mem Inst Oswaldo Cruz 2010; 105: 436–439.

65. Andrade ZA. A double and paradoxical role for angiogenesis. Rev Patol Trop 2013; 42: 259-264.

66. Abdel Fattah NS, Ahmed NS. Evidence of intra-hepatic vascular proliferation remodeling early after cure in experimental schistosomiasis *mansoni*: an immunohistochemical descriptive study. Exp Parasitol 2012; 130: 58–62.

67. Osman GY, Mohamed AH, Maghrabi OA, Elkenawy AE, Salem TA, Elmalawany AM. Immunohistochemical activities and anti-helminthic of blue green algae in *Schistosoma mansoni* infection in albino mice. RRJZS 2017; 5: 73-82.